J. Math. Anal. Appl. 366 (2010) 538–549

Contents lists available at ScienceDirect

Journal of Mathematical Analysis and Applications

www.elsevier.com/locate/jmaa

Analytical and numerical solution of a generalized Stefan problem exhibiting two moving boundaries with application to ocean delta formation

J. Lorenzo-Trueba, V.R. Voller *

Department of Civil Engineering, St. Anthony Falls Laboratory, University of Minnesota, Minneapolis, MN 55414, USA

ARTICLE INFO

Article history:
Received 24 June 2009
Available online 14 January 2010
Submitted by P. Broadbridge

Keywords:
Stefan problem
Dual moving boundaries
Sediment delta
Enthalpy solution
Similarity solution

ABSTRACT

A model associated with the formation of sedimentary ocean deltas is presented. This model is a generalized one-dimensional Stefan problem bounded by two moving boundaries, the shoreline and the alluvial-bedrock transition. The sediment transport is a non-linear diffusive process; the diffusivity modeled as a power law of the fluvial slope. Dimensional analysis shows that the first order behavior of the moving boundaries is determined by the dimensionless parameter $0 \leqslant R_{ab} \leqslant 1$—the ratio of the fluvial slope to bedrock slope at the alluvial-bedrock transition. A similarity form of the governing equations is derived and a solution that tracks the boundaries obtained via the use of a numerical ODE solver; in the cases where the exponent θ in the diffusivity model is zero (linear diffusion) or infinite, closed from solutions are found. For the full range of the diffusivity exponents, $0 \leqslant \theta \to \infty$, the similarity solution shows that when $R_{ab} < 0.4$ there is no distinction in the predicted speeds of the moving boundaries. Further, within the range of physically meaningful values of the diffusivity exponent, i.e., $0 \leqslant \theta \sim 2$, reasonable agreement in predictions extents up to $R_{ab} \sim 0.7$. In addition to the similarity solution a fixed grid enthalpy like solution is also proposed; predictions obtained with this solution closely match those obtained with the similarity solution.

1. Introduction

In a moving boundary problem one or more of the domain boundaries is an *a priori* unknown function of space and time. The classical example is the one phase Stefan melting problem [1] where one of the domain boundaries is the moving solid/liquid front. Generalizations of the Stefan problem have been applied to wide classes of problems. A Stefan like problem of current interest—dating back to the work of Swenson et al. [2] and Marr et al. [3]—is associated with the formation of sediment ocean deltas and fluvial sediment fans. For such systems, an analogy between sediment and heat transport can be effectively applied to arrive at a generalized Stefan problem that has some interesting features. In particular, the appearance of multiple moving boundaries; a feature also seen in some solidification [4–6] and polymer swelling systems [7].

Both analytical and numerical solutions have been developed for the sediment ocean delta problem. Under the conditions of a constant sediment flux applied at $x = 0$ and a constant bedrock slope, Voller et al. [8] developed a closed form similarity solution for a one-dimensional version of the sediment delta problem in which the moving boundary of interest is the shoreline (SHL) $x = s_{sh}(t)$. Capart and co-workers [9–11] and Lorenzo-Trueba et al. [12] expand on this work by developing analytical and semi-analytical solutions that track two moving boundaries, the seaward movement of the shoreline and the

* Corresponding author.
E-mail address: volle001@umn.edu (V.R. Voller).

0022-247X/$ – see front matter
doi:10.1016/j.jmaa.2010.01.008

landward movement of the alluvial-bedrock transition (ABT) $x = -s_{ab}(t)$. A feature in the analytical dual moving boundary treatments is the assumption of a linear diffusion law to model the sediment unit flux in terms of a constant diffusivity ν multiplied by the local slope of the sediment deposit, i.e.,

$$q(x) = -\nu \frac{\partial h}{\partial x} \tag{1}$$

where h is the sediment height above a horizontal datum and the units of the flux q are volumetric sediment bed transport per unit width and time; a definition that takes account for porosity in the sediment deposit.

A basic approximate solution to the dual moving boundary sediment delta problem can be obtained by assuming that the surface of the deposited sediment is linear. As detailed in Kim and Muto [13], this allows for the construction of a geometric relationship that can be used to track both the SHL and ABT. In more sophisticated approximate approaches numerical solutions, employing coordinated transforms have been presented by Parker and Muto [14], Swenson and Muto [15]. A feature in these works is the consideration of a non-linear model for the unit flux where the constant diffusivity ν in (1) is replaced by a function of the sediment deposit's slope, i.e.,

$$\nu = \nu^* \left| \frac{\partial h}{\partial x} \right|^{\theta} \tag{2}$$

where ν^* is a constant with dimensions of diffusivity and the exponent $\theta \geqslant 0$ is a constant.

A drawback of the coordinate transform numerical approaches for the sediment delta problem [14,15] is that there is not an obvious path toward the solution of two-dimensional problems. To address this, Voller et al. [16] develop an "enthalpy" like solution that can operate on a fixed grid in the untransformed space. This solution approach has been successfully verified with the single moving shoreline analytical solution of Voller et al. [8] and applied to the problems of the growth of two-dimensional deltas [16]. As the method stands, however, is not able to handle the simultaneous tracking of the SHL, $x = s_{sh}(t) > 0$, and the ABT, $x = s_{ab}(t) < 0$.

The objective of this paper is two-fold. In the first place the dual boundary delta growth similarity solution of Lorenzo-Trueba et al. [12] will be extended to allow for the non-linear diffusion form in (2). In the general case, $\theta > 0$, the resulting similarity ODE requires a numerical solution. In the special limit cases, $\theta = 0$ and $\theta \to \infty$, however, closed form solutions can be obtained. In the $\theta = 0$ limit, the error function closed form solution presented by Lorenzo-Trueba et al. [12] results. In the $\theta \to \infty$ limit, the geometrical solution of Kim and Muto [13] is obtained. Numerical treatment of the similarity equations indicates that the solution in the general case of finite non-zero value of θ is bounded by these two limit solutions.

The second objective of this paper is to further develop the enthalpy solution of Voller et al. [16] so that it can deal with the dual moving boundary delta growth problem under the assumption of the non-linear diffusion form in (2). This numerical approach is verified by comparing with the closed ($\theta = 0$) and numerical ($\theta > 0$) solutions of the similarity ODE.

2. The dual moving boundary problem

2.1. Equations

Following from previous work [12], a one-dimensional schematic of the problem of interest, a cross sectional view of a sediment delta building on a non-subsiding constant slope ($-\beta > 0$) bedrock into an ocean with a fixed relative sea-level $z = 0$, is shown in Fig. 1. Initially a constant unit sediment flux $q_0 > 0$ (area/time) is introduced upstream of the initial SHL position $x = 0$. The bedrock slope is sufficient to transport this sediment flux to the ocean where it deposits to form a small sediment wedge. Over time this sediment wedge increases in size, consisting of a submarine component advancing into the deepening ocean and a subaerial fluvial component moving landward, up the bedrock slope, see Fig. 1. When the downstream moving sediment flux on the bedrock encounters the upstream portion of the sediment wedge it begins to deposit. This deposition continues down the length of the fluvial surface. At the SHL the remaining flux is deposited offshore, contributing to the advance of the SHL. The sediment is moved and deposited over the fluvial surface by channel processes. Through the coupling of the momentum balance with fundamental descriptions of the sediment bed-load transport it can be argued, for a wide range of laboratory and field cases [14,15,17], that the sediment flux on the fluvial surface can be modeled by the general non-linear form given in (2). Depending on the assumptions made and situations considered values of the exponent in this model have been reported in the range $0 \leqslant \theta \sim 2$. To close the model, the mechanism for submarine sediment transport and deposition needs to be defined. In keeping with previous works [2,12] it is assumed that grain movement by subaqueous avalanches is much more rapid than the movement of sediment by the fluvial processes in the subaerial domain, and as such the offshore transport deposition can be modeled as a "sediment wedge" with a constant angle of repose with slope α.

With the above assumption for the sediment transport, a governing equation is derived by using the unit flux definition (1) in the Exner equation [18] for the mass balance in the sediment wedge, to arrive at the diffusion equation

$$\frac{\partial h}{\partial t} = \frac{\partial}{\partial x}\left(\nu^* \left| \frac{\partial h}{\partial x} \right|^{\theta} \frac{\partial h}{\partial x} \right), \quad s_{ab}(t) \leqslant x \leqslant s_{sh}(t). \tag{3}$$

The boundary conditions for this dual moving boundary problem are

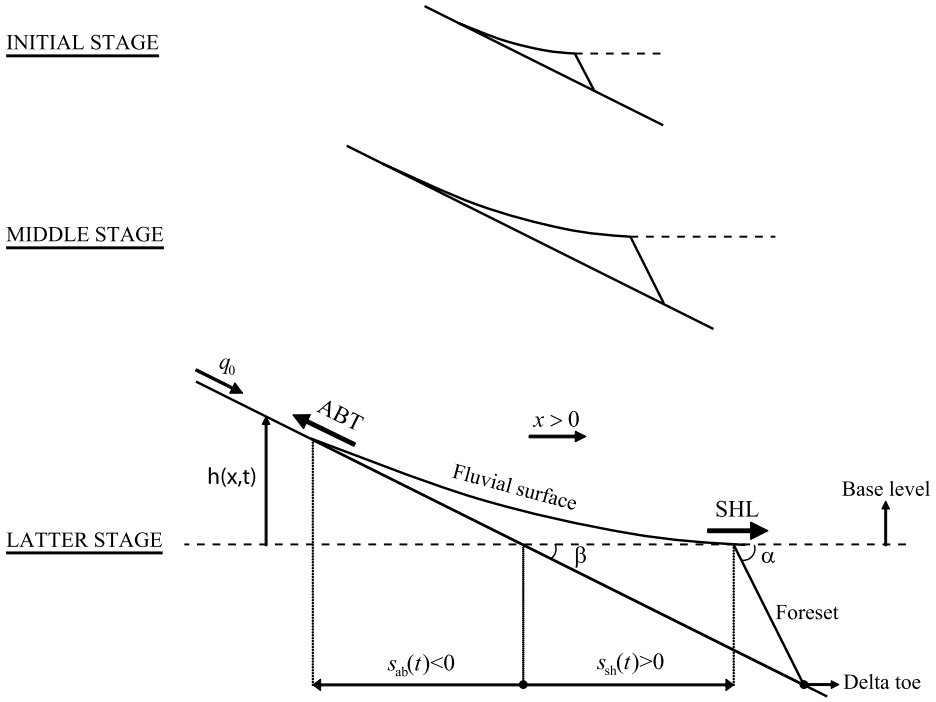

Fig. 1. Schematic of dual moving boundary problem; the shoreline (SHL) moves seaward, and the alluvial-bedrock transition (ABT) moves landward.

$$h|_{x=s_{ab}(t)} = -\beta s_{ab}(t), \tag{4a}$$

$$h|_{x=s_{sh}(t)} = 0, \tag{4b}$$

$$\nu^* \left|\frac{\partial h}{\partial x}\right|^{\theta} \frac{\partial h}{\partial x}\bigg|_{x=s_{ab}(t)} = -q_0, \tag{4c}$$

$$\nu^* \left|\frac{\partial h}{\partial x}\right|^{\theta} \frac{\partial h}{\partial x}\bigg|_{x=s_{sh}(t)} = -\gamma s_{sh} \frac{ds_{sh}}{dt} \tag{4d}$$

where the slope ratio $\gamma = \alpha\beta/(\alpha - \beta)$ is referred to as the effective submarine slope; the product γs_{sh} gives the depth of the ocean at the delta toe. The first condition (4a) fixes the upstream vertex of the sediment wedge to the height of the bedrock at the current position of the ABT. The second condition (4b) sets the SHL at sea-level. The extra boundary conditions (4c) and (4d) are required to track the positions of the unknown moving boundaries, the SHL $x = s_{sh}(t)$ and ABT $x = s_{ab}(t)$. The condition (4c) is a statement of the continuity of flux at $x = s_{ab}(t)$ and the condition (4d), analogous to the Stefan condition in heat transfer, expresses the sediment balance at the SHL. The appropriate initial conditions are $s_{sh}(0) = s_{ab}(0) = h(x, 0) = 0$.

2.2. Behavior in limit $\theta \to \infty$

At this point it is worthwhile briefly noting the behavior of the problem in (3) and (4) in the limit of a large value for the exponent θ in the non-linear diffusion model (2). First, based on the purely depositional nature of the system, the following behaviors that hold regardless of the value of θ are noted:

(i) the rate of deposition is finite and positive, $\partial h/\partial t > 0$, $\forall x \in [s_{ab}, s_{sh}]$, $t \geqslant 0$,
(ii) the velocity of the SHL ds_{sh}/dt is finite at any SHL position $s_{sh} > 0$,
(iii) the slope of the fluvial surface is bounded by $-\beta \leqslant \partial h/\partial x < 0$, $\forall x \in [s_{ab}, s_{sh}]$, $t \geqslant 0$.

Together, through (3), (4c), and (4d) these conditions imply that for any value of θ the value of sediment unit flux decreases monotonically between $x = s_{ab}$ and $x = s_{sh}$ and is bounded by

$$q_0 \geqslant -\nu^* \left|\frac{\partial h}{\partial x}\right|^{\theta} \frac{\partial h}{\partial x} \geqslant \gamma s_{sh} \frac{ds_{sh}}{dt}. \tag{5}$$

This in turn implies, through (iii) above, that the non-linear diffusion term $\nu = \nu^* |\partial h/\partial x|^{\theta}$ is strictly positive and bounded.

Further progress is made from these observations by using the fact that $|\partial h/\partial x| = -\partial h/\partial x$ to expand the right-hand side of (3) and arrive at

$$\frac{1}{(\theta+1)}\frac{\partial h}{\partial t} = \nu^* \left|\frac{\partial h}{\partial x}\right|^{\theta} \frac{\partial^2 h}{\partial x^2}, \quad s_{ab}(t) \leqslant x \leqslant s_{sh}(t). \tag{6}$$

Based on the observations made above, finite positive deposition and bounded non-linear diffusivity, it can be concluded from (6) that in the limit $\theta \to \infty$ the curvature of the fluvial surface $\partial^2 h/\partial x^2 \to 0$, i.e., the fluvial surface becomes linear. As a linear fluvial surface is approached the rate of deposition $\partial h/\partial t$ becomes a function of time alone and hence, with reference to (3), the flux term $\nu^*|\partial h/\partial x|^{\theta}\partial h/\partial x$ needs to approach a linear function in space. So in the limit of $\theta \to \infty$ both the fluvial surface and the flux become linear functions in space.

2.3. A dimensionless form

On defining the ratio of the fluvial to bedrock slope at the ABT to be

$$R_{ab} = -\frac{1}{\beta}\frac{\partial h}{\partial x}\bigg|_{x=s_{ab}}, \tag{7}$$

which through (4c) is a constant, appropriate dimensionless variables for the problem at hand can be defined as follows

$$x^d = \frac{x}{\ell}, \qquad h^d = \frac{h}{\beta\ell}, \qquad s^d = \frac{s}{\ell}, \qquad t^d = \frac{tq_0}{\ell^2\beta R_{ab}}, \tag{8}$$

where the superscript d indicates a dimensionless variable, and ℓ is a convenient length scale. In this way, dropping the d superscript for convenience of notation, the following dimensionless version of the governing equations (3) and (4) results

$$\frac{\partial h}{\partial t} = \frac{\partial}{\partial x}\left(\frac{1}{R_{ab}^{\theta}}\left|\frac{\partial h}{\partial x}\right|^{\theta}\frac{\partial h}{\partial x}\right), \quad s_{ab}(t) \leqslant x \leqslant s_{sh}(t) \tag{9}$$

with boundary conditions

$$h|_{x=s_{ab}(t)} = -s_{ab}(t), \tag{10a}$$

$$h|_{x=s_{sh}(t)} = 0, \tag{10b}$$

$$\frac{1}{R_{ab}^{\theta}}\left|\frac{\partial h}{\partial x}\right|^{\theta}\frac{\partial h}{\partial x}\bigg|_{x=s_{ab}(t)} = -R_{ab}, \tag{10c}$$

$$\frac{1}{R_{ab}^{\theta}}\left|\frac{\partial h}{\partial x}\right|^{\theta}\frac{\partial h}{\partial x}\bigg|_{x=s_{sh}(t)} = -R_{sh}s_{sh}\frac{ds_{sh}}{dt}. \tag{10d}$$

In the above

$$R_{sh} = \frac{\gamma}{\beta} = \frac{\alpha-\beta}{\alpha} \tag{11}$$

is the ratio of the effective submarine slope to the bedrock slope and

$$q^d = -\frac{1}{R_{ab}^{\theta}}\left|\frac{\partial h}{\partial x}\right|^{\theta}\frac{\partial h}{\partial x} \tag{12}$$

is identified as the dimensionless flux, $q^d = qR_{ab}/q_0$.

The dimensionless form (9) and (10) shows that the dual moving boundary problem related to the formation of an ocean sediment delta is fully specified by the value of the exponent in the non-linear diffusion law θ and the dimensionless parameters of the alluvial-bedrock slope ratio, R_{ab}, and the shoreline slope ratio, R_{sh}. For future reference, note that the value of the alluvial-bedrock slope ratio is theoretically bounded by $0 \leqslant R_{ab} \leqslant 1$ and the value of the shoreline slope ratio is restricted to be $R_{sh} \geqslant 1$.

2.4. Similarity equations

On setting the movement of the ABT and the SHL to be respectively

$$s_{ab} = -2\lambda_{ab}t^{\frac{1}{2}}, \tag{13a}$$

$$s_{sh} = 2\lambda_{sh}t^{\frac{1}{2}}, \tag{13b}$$

introducing the similarity variable

$$\xi = \frac{x}{2t^{\frac{1}{2}}} \tag{14}$$

and scaling the sediment height by

$$\eta = \frac{h}{2t^{\frac{1}{2}}}, \tag{15}$$

Eqs. (9) and (10) reduce to the ordinary differential equation

$$\frac{1}{2}\frac{d}{d\xi}\left(\frac{1}{R_{ab}^{\theta}}\left|\frac{d\eta}{d\xi}\right|^{\theta}\frac{d\eta}{d\xi}\right) + \xi\frac{d\eta}{d\xi} - \eta = 0, \quad -\lambda_{ab} \leqslant \xi \leqslant \lambda_{sh} \tag{16}$$

with

$$\eta|_{\xi=-\lambda_{ab}} = \lambda_{ab}, \tag{17a}$$

$$\eta|_{\xi=\lambda_{sh}} = 0, \tag{17b}$$

$$\frac{1}{R_{ab}^{\theta}}\left|\frac{\partial\eta}{\partial\xi}\right|^{\theta}\frac{d\eta}{d\xi}\bigg|_{\xi=-\lambda_{ab}} = -R_{ab}, \tag{17c}$$

$$\frac{1}{R_{ab}^{\theta}}\left|\frac{\partial\eta}{\partial\xi}\right|^{\theta}\frac{d\eta}{d\xi}\bigg|_{\xi=\lambda_{sh}} = -2R_{sh}\lambda_{sh}^{2}. \tag{17d}$$

In application it is worth noting that since $\partial\eta/\partial\xi$ is always negative the term $|\partial\eta/\partial\xi|$ can be replaced with the more convenient term $(-\partial\eta/\partial\xi)$.

3. Analytical and numerical solution methods

3.1. Closed form solutions for the similarity equations

Two closed form solutions of the similarity statement of the problem (16) to (17) can be identified. The first at $\theta = 0$, and the second in the limit $\theta \to \infty$. The case $\theta = 0$ has been previously been investigated by Capart and co-workers [9–11] and Lorenzo-Trueba et al. [12]. A full derivation is given in Lorenzo-Trueba et al. [12]. In brief, in this limit, the solution of (16) satisfying (17b) and (17c) is

$$\eta(\xi) = R_{ab}\left[\lambda_{sh}\left(\frac{e^{-\xi^2} + \pi^{\frac{1}{2}}(\xi erf(\xi) + erf(\lambda_{ab}))}{e^{-\lambda_{sh}^2} + \pi^{\frac{1}{2}}\lambda_{sh}(erf(\lambda_{ab}) + erf(\lambda_{sh}))}\right) - \xi\right]. \tag{18}$$

On substituting this relationship into (17a) and (17d) the following non-linear equations in λ_{ab} and λ_{sh} can be obtained

$$\frac{R_{ab}e^{-\lambda_{sh}^2}}{e^{-\lambda_{sh}^2} + \pi^{\frac{1}{2}}\lambda_{sh}(erf(\lambda_{ab}) + erf(\lambda_{sh}))} - 1 = 2\lambda_{sh}^2 R_{sh}, \tag{19a}$$

$$\frac{R_{ab}e^{-\lambda_{ab}^2}}{e^{-\lambda_{sh}^2} + \pi^{\frac{1}{2}}\lambda_{sh}(erf(\lambda_{ab}) + erf(\lambda_{sh}))} = \frac{\lambda_{ab}}{\lambda_{sh}}(1 - R_{ab}). \tag{19b}$$

To arrive at the second closed solution in the limit $\theta \to \infty$, we first note that, by discussion above, in this limit the fluvial surface and the sediment flux approach linear functions of space, i.e.,

$$\lim_{\theta\to\infty}\eta = R_{ab}(\lambda_{sh} - \xi), \tag{20}$$

$$\lim_{\theta\to\infty}\frac{1}{R_{ab}^{\theta}}\left|\frac{d\eta}{d\xi}\right|^{\theta}\frac{d\eta}{d\xi} = -R_{ab} - \frac{\xi + \lambda_{ab}}{\lambda_{sh} + \lambda_{ab}}\left(2\lambda_{sh}^2 R_{sh} - R_{ab}\right). \tag{21}$$

The profile in (20) automatically satisfies the fixed elevation condition at the SHL (17b) and by construction the sediment flux in (21) satisfies the flux conditions in both (17c) and (17d). In order to satisfy the remaining elevation condition (17a) the moving boundary parameters need to be constrained by the relationship

$$\lambda_{ab} = \left[\frac{R_{ab}}{1 - R_{ab}}\right]\lambda_{sh}. \tag{22}$$

In this way, the limit values on the right-hand sides of (20) and (21) satisfy the boundary conditions but to complete the solution they must also satisfy the governing equation (16). On substitution of the right-hand sides of (20) and (21) into (16) it is seen, after some manipulation using (22), that the governing equation is satisfied if the condition

$$\lambda_{sh} = \sqrt{\frac{\frac{1}{2}R_{ab}(1-R_{ab})}{R_{sh}(1-R_{ab})+R_{ab}}} \tag{23}$$

is met. Eqs. (22) and (23) match the solution generated by Kim and Muto [13] from geometric arguments alone. Hence, the purely geometric solution of Kim and Muto [13] is in fact the $\theta \to \infty$ limit solution of the diffusion model given in (3) and (4).

3.2. Numerical solution of the similarity equations

For the general case of a finite non-zero value of θ, the similarity equations (16) and (17) can also be solved numerically. This involves an iterative approach with the following steps.

(i) For the chosen values of θ, R_{ab}, and R_{sh}, initial estimates of λ_{ab} and λ_{sh} are obtained from an approximate. The geometric solution (22) and (23) can be used to get an initial guess.
(ii) Then Eq. (16) along with the boundary conditions (17b) and (17c) is solved using the bvp4c routine in Matlab [19].
(iii) The boundary conditions (17a) and (17d) are then used to update the guesses for λ_{ab} and λ_{sh}; an under-relaxation of 0.25 is used.
(iv) Steps (ii) and (iii) are repeated until convergence; declared when the change in the sum of λ_{ab} and λ_{sh} between iterations falls below 10^{-5}.

This basic approach works well for values of $R_{ab} \leqslant 0.9$. To achieve convergence at larger values of θ and values of R_{ab} that approach unity care needs to be taken in running the solver, e.g., choosing the initial guess.

3.3. A fixed grid numerical solution

In addition to the numerical solution of the similarity equations a numerical solution of the problem in the physical space can also be developed. Such a solution is seen as having the advantage of being able to operate in cases where similarity does not hold. The solution used here is an adaptation of the fixed grid "enthalpy" like solution proposed by Voller et al. [16] for modeling linear diffusion sediment transport problems with a single moving boundary.

As a proxy for the enthalpy of heat transfer solutions we define total sediment in the system as

$$H = \begin{cases} h + L(x), & h > 0, \\ 0, & h = 0 \end{cases} \tag{24}$$

where, taking account of the dimensionless variable definitions in (8), L is the dimensionless depth of the ocean at the delta toe when the SHL is at x, i.e.,

$$L = \begin{cases} 0, & x < 0, \\ x \cdot R_{sh}, & x \geqslant 0. \end{cases} \tag{25}$$

With this definition we can write down a single Exner sediment balance equation for the full solution space as

$$\frac{\partial H}{\partial t} = \frac{\partial}{\partial x}\left(q^d\right), \quad -\infty \leqslant x \leqslant \infty \tag{26}$$

where

$$q^d = \min\left(-\frac{1}{R_{ab}^{\theta}}\left|\frac{\partial h}{\partial x}\right|^{\theta}\frac{\partial h}{\partial x}, R_{ab}\right) \tag{27}$$

and, inverting (24),

$$h = \max(H - L, 0). \tag{28}$$

The boundary conditions for (26) are

$$\lim_{x\to-\infty} q^d = R_{ab} \quad \text{and} \quad \lim_{x\to\infty} h = 0 \tag{29}$$

and the initial conditions are

$$H = h = \begin{cases} x, & x < 0, \\ 0, & x \geqslant 0. \end{cases} \tag{30}$$

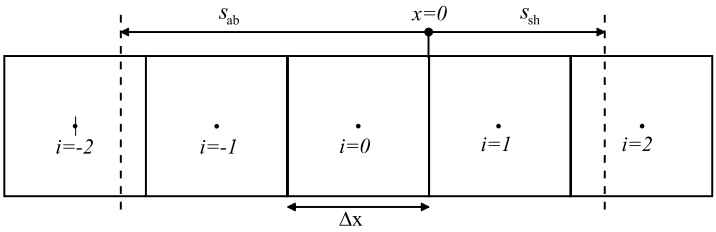

Fig. 2. The discrete domain. In general the shoreline and the alluvial-bedrock transition positions, s_{sh} and s_{ab} respectively, are in between two nodes of our discrete domain.

The one-dimensional discretization illustrated in Fig. 2 is used to develop a numerical solution of Eq. (24) to (30). Note that (i) this discretization is based on a uniform grid size Δx, (ii) that the origin point $x = 0$ is located at the interface between two nodes, (iii) the first landward node is indexed $i = 0$, (iv) as we move seaward the node index increases ($i = 1, 2, 3 \ldots$) and (v) as we move landward the node index decreases ($i = 0, -1, -2 \ldots$). In this way the location of any node is given by $x = (i - 0.5) \cdot \Delta x$.

On the domain in Fig. 2 the explicit time integration finite difference form of (24) is

$$H_i^{new} = H_i + \frac{\Delta t}{\Delta x} \cdot \left(q^d_{i+\frac{1}{2}} - q^d_{i-\frac{1}{2}}\right) \tag{31}$$

where the superscript *new* refers to values at the new time step, subscript $i + 1/2$ refers to the interface between nodes i and $i + 1$, and the flux from node i to node $i + 1$ is approximated as

$$q^d_{i+\frac{1}{2}} = \min\left(\frac{1}{R^\theta_{ab}}\left|\frac{h_{i+1} - h_i}{\Delta x}\right|^\theta \left(\frac{h_i - h_{i+1}}{\Delta x}\right), R_{ab}\right). \tag{32}$$

Note since the slope $|\partial h/\partial x|$ is bounded above by R_{ab} the maximum value for the non-linear diffusivity in the system

$$\nu = \frac{1}{R^\theta_{ab}}\left|\frac{h_{i+1} - h_i}{\Delta x}\right|^\theta \tag{33}$$

cannot exceed unity. Therefore positive coefficient and hence a reasonable guarantee of stability will be established if the time and space steps are chosen such that $\Delta t/\Delta x^2 < 0.5$. In addition to stability considerations it is also noted that to retain accuracy the switching of the interface flux $q^d_{i+\frac{1}{2}}$, from the input value R_{ab} to one controlled by the fluvial surface, Eq. (32), needs to take place at a frequency larger than the simulation time step. In meeting these stability and accuracy conditions the simulations in the current work use a space step $\Delta x = 1$ and a time step in the range $0.01 \leqslant \Delta t \leqslant 0.05$.

At each time step solution of (31) will explicitly provide new values for the nodal values of the total sediment H^{new}. From this field new time step values for the sediment heights h_i^{new} are calculated from the discrete form of (28). This provides sufficient information to recalculate the fluxes in (32) and propagate the solution of (31) forward in time.

Although not required as part of the solution process, at each time step the location of the SHL and ABT can be estimated with the following steps. For the SHL ($i > 0$) the current total sediment field H_i is searched, and the unique node i where $0 < H_i < L_i$ is located. The SHL position is then determined by interpolation through the control volume around node i, i.e.,

$$s_{sh} = (i - 1)\Delta x + \frac{H_i}{L_i}\Delta x. \tag{34}$$

For the ABT a search is made through the nodes in the order $i = 0, -1, -2 \ldots$ until the first node where the upstream flux $q^d_{i-1/2}$ is, by (32), calculated as R_{ab}. The ABT position is then determined by interpolation between nodes i and $i - 1$

$$s_{ab} = \frac{h_i - R_{ab}(0.5 - i)\Delta x}{1 - R_{ab}}. \tag{35}$$

4. Results

4.1. Similarity solution

The solution of the similarity solution is fully determined by the specification of the alluvial-bedrock slope ratio, R_{ab}, and the shoreline slope ratio, R_{sh}. Our interest is to explore the consequence of the various solutions methods presented under conditions that match those in the field. In this setting the foreset slope, α, is typically much greater than the bedrock slope, β, hence through (11) it is reasonable to always assume a value $R_{sh} = 1$. In contrast the value of R_{ab} could vary across the full theoretical range $0 \leqslant R_{ab} \leqslant 1$; typically observed field values are in the range $0.2 \leqslant R_{ab} \leqslant 0.8$ (see discussion in [12]). In this way the results from the similarity solution are best presented by fixing $R_{sh} = 1$ and plotting the

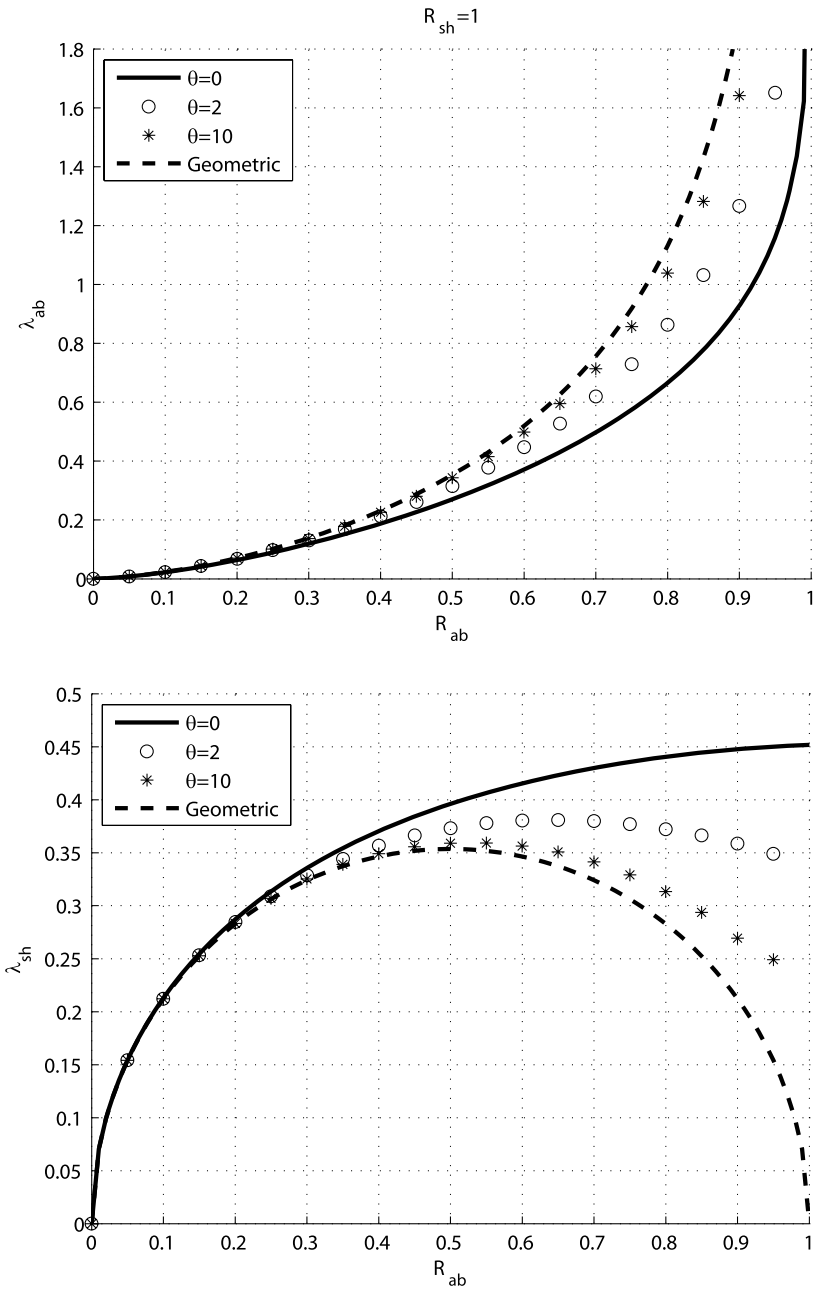

Fig. 3. The solution space for the moving boundary parameters λ_{ab} (ABT) and λ_{sh} (SHL).

values of the moving boundary parameters λ_{ab} and λ_{sh} against $0 \leqslant R_{ab} \leqslant 1$. Fig. 3 shows these plots for the cases where $\theta = 0, 2, 10, \infty$. Predictions for the finite values of θ are obtained from the ODE solution of (16) and (17). Note, however, the $\theta = 0$ solution obtained in this manner is indistinguishable from the values obtained from the closed form analytical solution (19). The $\theta \to \infty$ solution is obtained from the geometric solution in (22) and (23).

Some key observation on the predicted behaviors are made.

(i) All the solutions are bounded by geometric, $\theta \to \infty$, and linear diffusion, $\theta = 0$ models.
(ii) In the range $0 < R_{ab} < 0.4$ the predicted values of lam λ_{ab} and λ_{sh} are not affected by the value of diffusive exponent θ.
(iii) There is a convergence tendency in the similarity solution predictions to the geometric solution as the value θ increases.
(iv) The value of λ_{sh} that controls the shoreline advance is only monotonic for the linear diffusion case, $\theta = 0$. For all other values there is a decrease in this value at high values of R_{ab}. In the geometric model, $\theta \to \infty$, this value goes to zero as R_{ab} approaches 1 indicating an immobile SHL.

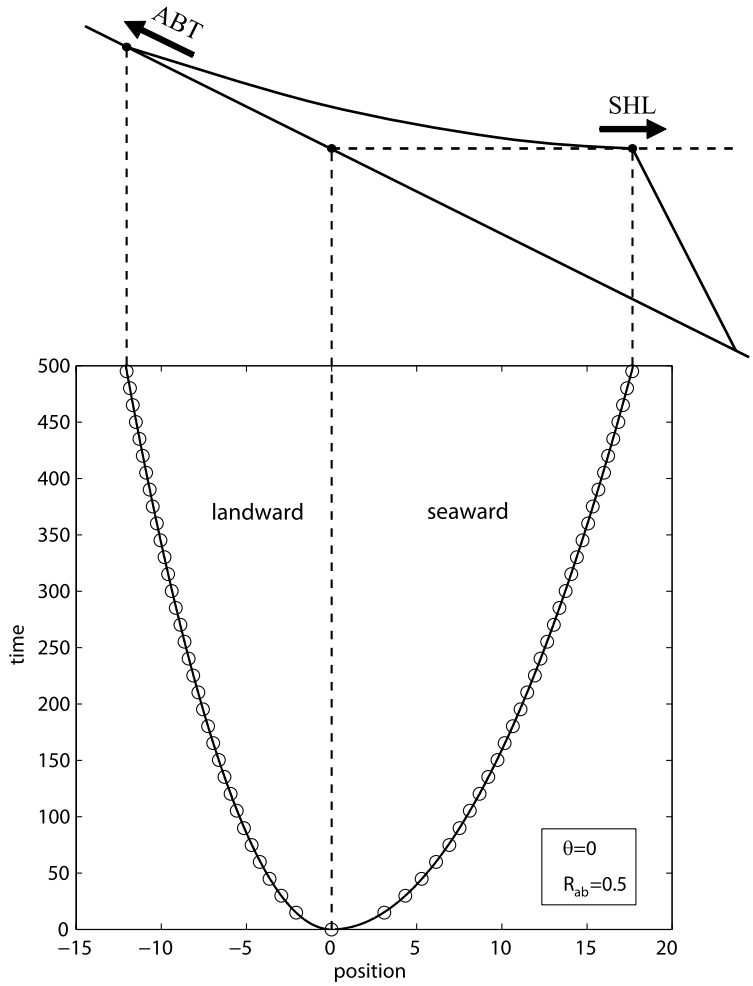

Fig. 4. Comparison between enthalpy solution (open circles) and similarity solution (continuous line). The sketch on top represents the longitudinal profile at the latest time in the graph.

(v) There is a marked sensitivity in the predictions for ABT parameter λ_{ab} as larger values of R_{ab} are approached. The geological consequences of this feature is extensively discussed in the linear diffusion analysis recently precedent by Lorenzo-Trueba et al. [12].

4.2. Enthalpy solution

The enthalpy method provides an accurate approximation of the similarity solution. For a range of θ and R_{ab} values, Figs. 4 and 5 show plots of the movement of the SHL and ABT with time. In all cases a close match between the similarity and the enthalpy predictions is observed.

A further test of the robustness of the enthalpy solution is revealed by investigating its performance when θ approaches a large value. Fig. 6 shows predictions of the SHL and ABT movements when $\theta = 200$. As predicted by the theory this enthalpy solution closely matches the geometric model predictions from (22) and (23).

5. Discussion

As noted in the introduction of this paper, depending on the situation considered and the semi-empirical sediment transport laws used experiments [12,17] and theoretical models [12,14,15,17] report the diffusive exponent to be in the range $0 \leqslant \theta \sim 2$. Currently there is no consensus on a single correct value for use in modeling "real world systems" [17]. Experiments underscore this point. Lorenzo-Trueba et al. [12] recover accurate comparisons with experimental delta growth models using an analytical solution based on a linear diffusion law $\theta = 0$. In contrast, reported comparison between numerical models and delta building experiments [14,15] show a best fit when $0.95 \leqslant \theta \leqslant 1.25$. Finally in analyzes of a delta

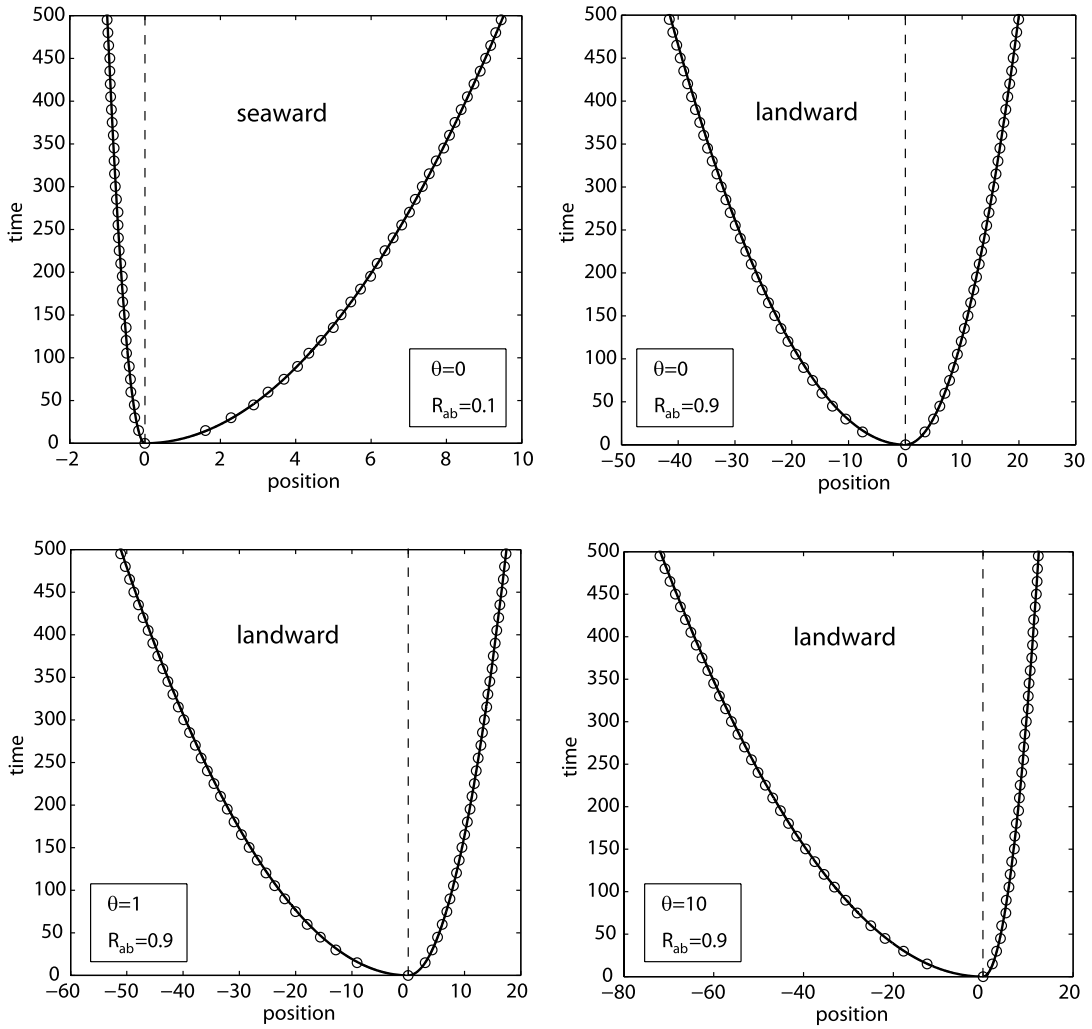

Fig. 5. Further comparisons between enthalpy (open circles) solution and similarity solution (continuous line).

depositing system in a fixed domain (no ABT or SHL moving boundaries) Postma et al. [17], in fitting to a transient nonlinear diffusion model, obtain values of $\theta \sim 2$. In this respect a striking feature of the results in Fig. 3 is that while $R_{ab} < 0.7$, deviations between the $\theta = 0$ and $\theta = 2$ predictions of the moving boundary parameters λ_{ab} and λ_{sh} are below 10%. Taking into account the field and experimental difficulties in accurately measuring R_{ab} and other ambiguities in the system such as porosity [12] these deviations may not be significant. Hence, it is reasonable to suggest that for values $R_{ab} \leqslant 0.7$ the modeling detail of choosing the "correct" value of the exponent for θ in (2) will make no qualitative difference to the boundary movement predictions and have only a marginal influence on quantitative values. It is not until we move beyond $R_{ab} = 0.7$—approaching the upper limit for field observations—that care may be required in identifying the appropriate value for the exponent θ.

Experimental systems of delta building processes (e.g., see figures in [12]) often exhibit what on first inspection appears to be a linear profile. This suggests that the simple geometric model ($\theta \to \infty$) should be a sound approach. The results in Fig. 3 confirm that this is more than reasonable provided that $R_{ab} \leqslant 0.4$. As we move beyond this value, however, there is a dramatic departure between the geometric prediction for λ_{ab} and λ_{sh}, and those obtained with "physically reasonable" values for the diffusivity exponent $0 \leqslant \theta \sim 2$. Hence, in terms of retaining quantitative predictions use of the geometric model may only begin to err when higher values R_{ab} are encountered. Nevertheless, due to the almost exact agreement between all models at values of $R_{ab} \leqslant 0.4$ and its profound simplicity, in qualitative studies of delta building processes use of the geometric model could be recommended.

Finally we note that the excellent comparison of the enthalpy and analytical solutions across the full range of θ and R_{ab} values is very encouraging. As noted above the enthalpy method has the most utility in developing solutions in more than one-dimension.

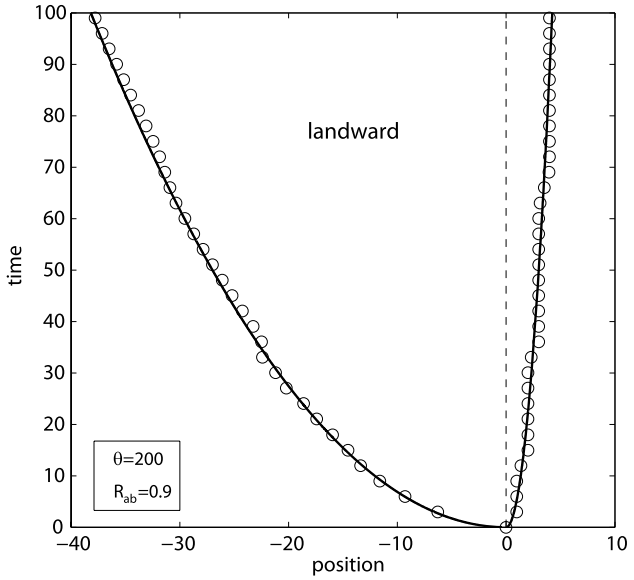

Fig. 6. Comparison between enthalpy solution with $\theta = 200$ (open circles) and geometric solution $\theta \to \infty$ (continuous line) for $R_{ab} = 0.9$.

6. Conclusions

This paper has presented a generalized Stefan problem related to the formation of a sediment ocean delta. Ingredients in this problem are a non-linear diffusivity related to the fluvial slope through the power law $\nu = \nu^* |\partial h/\partial x|^\theta$ and the appearance of two moving boundaries, the shoreline (SHL) and the alluvial-bedrock transition (ABT).

In terms of analysis, the key contribution has been to develop a similarity form and solution for the delta problem. In the limit of a linear diffusion $\theta = 0$ this solution recovers a recently derived closed form analytical solution [12]. At the other extreme, as $\theta \to \infty$, a closed form solution that matches the solution derived from geometric arguments is obtained.

In addition to the similarity solutions a fixed grid enthalpy like numerical solution of the delta problem has been proposed. Predictions from this solution have been shown to closely match those of the similarity solution. The utility of the enthalpy solution is that it can be applied to situations where similarity will not hold (e.g., more general non-linear diffusive terms) and to multi-dimensional cases.

The results in this paper also have some important geological consequence. First in interpreting field stratigraphy of ocean delta deposits, there may be no need to be concerned about choosing the most appropriate value of the diffusive exponent from the physical meaningful range $0 \leqslant \theta \sim 2$. Provided the alluvial-bedrock ratio $R_{ab} < 0.7$—near the upper end of observations—the differences in SHL and ABL predicted are well within the ambiguities in the system. Further, since in the range $R_{ab} < 0.4$ there is essentially no difference between the diffusion models and the geometric model, in developing qualitative models of the formation of sediment ocean deltas, due to its relative simplicity, the geometric model should be favored.

Further work will look toward developing the enthalpy approach to situations outside of the scope of the similarity solution and toward building a description of delta growth that takes into consideration additional features such as sea-level rise and bio-geochemical processes. A model with this capability will be invaluable in developing our understanding for costal restorations associated with the Gulf of Mexico.

Finally we note that in the current work a closed form solution for the similarity solution has only been found for the special cases of $\theta = 0$, and $\theta \to \infty$. Further analysis work will explore the possibility of finding solutions for finite and positive values of θ; perhaps by exploiting recent developments in the application of Lie symmetry methods to Stefan problems [20].

Acknowledgments

This work was supported by the STC program of the National Science Foundation via the National Center for Earth-surface Dynamics under the agreement Number EAR-0120914. The authors of grateful for fruitful discussion and input from Chris Paola, University of Minnesota; John Swenson, University of Minnesota Duluth; and Wonsuk Kim, University of Texas.

References

[1] J. Crank, Free and Moving Boundary Problems, Clarendon Press, Oxford, UK, 1984.
[2] J.B. Swenson, V.R. Voller, C. Paola, G. Parker, J.G. Marr, Fluvio-deltaic sedimentation: a generalized Stefan problem, European J. Appl. Math. 11 (2000) 433–452.

[3] J.G. Marr, J.B. Swenson, C. Paola, V.R. Voller, A two-diffusion model of fluvial stratigraphy in closed depositional basins, Basin Research 12 (2000) 381–398.
[4] V.R. Voller, A similarity for the solidification of multicomponent alloys, J. Heat Mass Transfer 40 (1997) 2869–2877.
[5] P. Tritscher, P. Broadbridge, A similarity solution of a multiphase Stefan problem incorporating general non-linear heat conduction, Int. J. Heat Mass Transfer 37 (1994) 2113–2121.
[6] M.G. Worster, Solidification of an alloy from a cooled boundary, J. Fluid Mech. 167 (1986) 481–501.
[7] S.I. Barry, J. Caunce, Exact and numerical solutions to a Stefan problem with two moving boundaries, Appl. Math. Model. 32 (2008) 83–98.
[8] V.R. Voller, J.B. Swenson, C. Paola, An analytical solution for a Stefan problem with variable latent heat, Intl. J. Heat Mass Transfer 47 (2004) 5387–5390.
[9] H. Capart, M. Bellal, D.L. Young, Self-similar evolution of semi-infinite alluvial channels with moving boundaries, J. Sediment. Res. 77 (2007) 13–22.
[10] S.Y.J. Lai, H. Capart, Two-diffusion description of hyperpycnal deltas, J. Geophys. Res. 112 (2007) F03005, doi:10.1029/2006JF000617.
[11] S.Y.J. Lai, H. Capart, Reservoir infill by hyperpycnal deltas over bedrock, Geophys. Res. Lett. 36 (2009) L08402, doi:10.1029/2008GL037139.
[12] J. Lorenzo-Trueba, V.R. Voller, T. Muto, W. Kim, C. Paola, J.B. Swenson, J. Fluid Mech. 628 (2009) 427–443.
[13] W. Kim, T. Muto, Autogenic response of alluvial-bedrock transition to base-level variation: Experiment and theory, J. Geophys. Res. 112 (2007) F03S14, doi:10.1029/2006JF000561.
[14] G. Parker, T. Muto, One-dimensional numerical model of delta response to rising sea-level, in: Proceedings of the Third IAHR Symposium, River, Coastal and Estuarine Morphodynamics, Barcelona, Spain, 2003, pp. 558–570.
[15] J.B. Swenson, T. Muto, Response of coastal plain rivers to falling relative sea-level: allogenic controls on the aggradational phase, Sedimentology 54 (2007) 207–221.
[16] V.R. Voller, J.B. Swenson, W. Kim, C. Paola, An enthalpy method for moving boundary problems on the earth's surface, Internat. J. Numer. Methods Heat Fluid Flow 16 (2006) 641–654.
[17] G. Postma, M.G. Kleinhans, P.Th. Meijer, J.T. Eggenhuisen, Sediment transport in analogue flume models compared with real world sedimentary systems: a new look at scaling sedimentary systems evolution in a flume, Sedimentology 55 (2008) 1541–1557.
[18] C. Paola, V.R. Voller, A generalized Exner equation for sediment mass balance, J. Geophys. Res. 110 (2005) F04014, doi:10.1029/2004JF000274.
[19] J. Kierzenka, L.F. Shampine, A BVP solver based on residual control and the Matlab PSE, ACM Trans. Math. Software 27 (2001) 299–316.
[20] R. Cherniha, S. Kovalenko, Exact solutions of nonlinear boundary value problems of the Stefan type, J. Phys. A: Math. Theor. 42 (2009) 355202, doi:10.1088/1751-8113/42/35/355202.